Proceedings of HT/FED 04
2004 ASME Heat Transfer/Fluids Engineering Summer Conference
July 11-15, 2004, Charlotte, NC

HT-FED2004-56362

ANALYSIS OF MELTING IN A SINGLE-COMPONENT METAL POWDER BED SUBJECT TO CONSTANT HEAT FLUX HEATING

Bin Xiao and Yuwen Zhang
Department of Mechanical and Aerospace Engineering
University of Missouri-Columbia
Columbia, MO-65211

ABSTRACT

To model Selective Laser Sintering (SLS) of single-component metal powders, melting of a subcooled powder bed with single-component metal powder is investigated analytically. Since laser processing of metal powder is a very rapid process, the liquid and solid phases of a partially molten powder particle may have different temperatures: the temperature in the liquid phase is higher than the melting point, and the temperature in the solid phase is below the melting point. Therefore, the local temperature of regions with partial molten particles is within a range of temperature adjacent to the melting point, instead of at melting point. In addition, the powder bed experiences a significant density change during melting. Therefore, melting of a metal powder bed can be modeled as a melting that occurs in a range of temperature with significant density change. The temperature distributions and locations of the various interfaces were obtained by solving the governing equations for solid, liquid and mushy zones in a one-dimensional system using an integral approximate method. The effects of porosity, sub-cooling, dimensionless thermal conductivity of gas, and dimensionless heat flux on the surface temperature and locations of the interfaces were investigated.

Nomenclature

c_p specific heat, ($J/kg^\circ C$)

f mass fraction of solid

f_0 mass fraction of solid on the heating surface

$h_{s\ell}$ latent heat of melting or solidification, (J/kg)

k thermal conductivity ($W/m\cdot K$)

K dimensionless thermal conductivity

q'' strength of line heat source (W/m)

s_0 location of heating surface (m)

s_m location of interface between constant porosity and constant volume regions (m)

s location of interface between solid zone and mushy zone (m)

S_0 dimensionless location of heating surface

S_m dimensionless location of interface between constant porosity and constant volume regions

S dimensionless location of interface between solid and mushy zones

T temperature ($^\circ C$)

t time (s)

V volume (m^3)

w velocity induced by shrinkage (m/s)

W dimensionless velocity induced by shrinkage

z vertical coordinate (m)

Z dimensionless vertical coordinate

Greek symbol

α thermal diffusivity (m^2/s)

δ thermal penetration depth (m)

θ dimensionless temperature

θ_0 dimensionless temperature on the heating surface

Δ dimensionless thermal penetration depth

ΔT one-half of phase change temperature range

ε volume fraction of void (porosity for unsintered powder), $(V_g + V_l)/(V_g + V_l + V_s)$

ρ density (kg / m^3)

τ dimensionless time

φ volume fraction

Subscripts

eff effective

g gas

f fusion

m mushy zone

p metal powder

s solid

INTRODUCTION

Selective laser sintering (SLS) is a rapid prototyping technology that creates three-dimensional freeform objects directly from the CAD design. An object is created by selectively consolidating a powder with a scanning laser beam layer by layer [1-2]. SLS has the capability of producing structurally sound parts directly from polymer, nylon, metal, and ceramics. The feasibility of producing metal parts directly by SLS has been analyzed with different metal systems [3-5]. In contrast to amorphous powders, metals do not exhibit softening but have a generally much higher melting temperature. Therefore melting and resolidification are the only mechanisms feasible for SLS processing of metals [6-7].

In the laser sintering of metal powders, scanning is carried out line by line and the energy causes melting along a row of powder particles on the heating surface. The tensile traction on the melt is not sufficient to confine the molten track to tubular shape, thus leading to the formation of a series of spheres with diameters similar to that of the laser beam. This phenomenon is called "balling" and it causes poor quality final products. A two-component powder approach that uses mixture of two metal powders with significantly different melting points can be used to overcome balling effects. Many fundamentals of which method have been investigated in recent years [8-10]. Since the SLS two-component metal powder uses two different materials, the weaker physical properties of the two powders often prevail in the final products. To fabricate the fully densified part using single metal powder, Meiners et al. [11] proposed Selective Laser Powder Remelting (SLPR), which is evolved from SLS. The powder particles are completely melted and a tubular shape can be formed after a single line scanning of the laser beam. This process of directly fabricating parts using single component metal powder by complete remelting is also referred to as Direct SLS of metal powder [12-13], Direct Metal SLS (DMSLS) [14] and Direct Metal Laser Remelting (DNLR) [15]. The techniques described in Ref. [11-15] require a very high laser intensity since the entire layer must be melted.

The balling phenomenon that is encountered in the SLS of single-component metal powder can also be overcome by allowing only a fraction of the powder to be melted under irradiation of the laser beam [16]. The partially molten powder particles bond together due to solidification of the partially molten powder particles when the laser beam moves away. Since the laser processing of metal powder is a very rapid process, the liquid and solid phases of a partially molten powder particle may have different temperatures: the temperature in the liquid phase is higher than the melting point while the temperature in the solid phase is below the melting point. Therefore, the local temperature of the regions with partial molten particles is within a range of temperature adjacent to the melting point, instead of at melting point.

Fundamentals of melting phenomena and its applications have been intensively investigated during the past years and detailed reviews are available in the literature [17-18]. The distinctive feature of melting occurred in the SLS process is that the powder bed experiences a significant density change due to shrinkage. This paper models melting of single-component metal powder bed as melting occurs in a range of temperature with significant density change. In this article an integral approximate method is used to solve the temperature distributions and locations of the various interfaces. Effects of porosity, sub-cooling and non-dimensional thermal conductivity will be investigated.

PHYSICAL MODEL

Figure 1 shows the physical model of melting of single-component metal powder. A powder bed with a uniform initial temperature, T_i, below the melting point of the metal powder, T_f, is in a half space, $z > 0$. Porosity of the powder bed during SLS is defined as the total volume of void, including the volumes of gas and liquid, relative to the total volume of the powder bed, i.e., $\varepsilon = \varphi_g + \varphi_l$, where, φ_g is the volume fraction of the gas in the powder bed and φ_l is the volume fraction of the liquid. The variation of porosity during different melting stages, as will be explained below, is different.

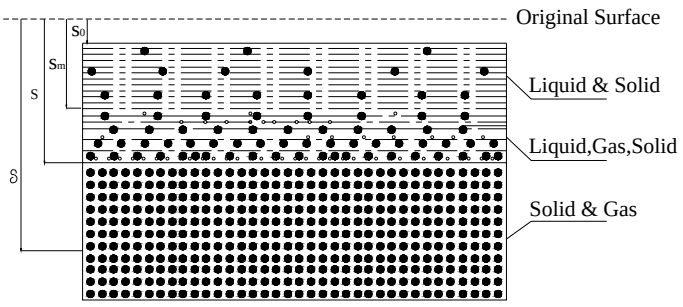

Fig. 1 Physical model

At time $t = 0$, a constant heat flux, $q^{"}$, is suddenly applied to the surface of the powder bed. Since the initial temperature of the powder bed is below the melting point, no melting occurs and the problem is a pure conduction problem with boundary conditions of the second kind. The melting starts at time $t = t_m$ when the surface temperature of the powder bed is at the lower limit of the phase change temperature range, $T_f - \Delta T$. There are two stages in the melting process. In the first melting stage $(t_m \le t < t_1)$, a mushy zone including solid, liquid and gas is formed. The porosity during the first stage of melting remains constant while volume of the powder bed continuously changes because the gas is driven out by the liquid generated during melting. The second stage of melting starts from time $t = t_1$ when the volume fraction of gas on the heating surface becomes zero. The mushy zone during the second stage of melting is divided into two parts: an upper part whose volume remains constant because the surface of the powder bed moves with the same shrinking velocity, a lower part whose porosity remains constant as it happens in the first stage. In addition, the following assumptions are made:

(1) The thermal properties of the powder are the same for both solid and liquid phases.
(2) The initial distribution of the volume fraction of the powder is uniform in the bed.

During preheating

During preheating, pure conduction heat transfer occurs in the powder bed. The energy equation and corresponding initial and boundary conditions for the preheating problems are

$$k_s \frac{\partial^2 T_s}{\partial z^2} = (1-\varepsilon)(\rho c)_P \frac{\partial T_s}{\partial t} \qquad 0 \le z < \infty, t < t_m \tag{1}$$

$$-k_s \frac{\partial T_s}{\partial z} = q^{"} \qquad z = 0,\ t < t_m \tag{2}$$

$$T_s = T_i \qquad z \to \infty,\ t < t_m \tag{3}$$

where k_s is the effective thermal conductivity in the powder bed [9].

The first melting stage

When melting first starts, the whole powder bed is divided into two parts: one is the mushy zone with constant porosity and the other is unsintered zone. Energy and continuity equations in the mushy zone are

$$\frac{\partial(\rho_m c_m T_m)}{\partial t} + \frac{\partial(\rho_m c_m w T_m)}{\partial z} = \frac{\partial}{\partial z}(k_m \frac{\partial T_s}{\partial z}) + \rho_m h_{sl} \frac{\partial f}{\partial t}$$
$$s_0(t) < z < s(t),\ t_m < t < t_1 \tag{4}$$

$$\frac{\partial \rho_m}{\partial t} + \frac{\partial(\rho_m w)}{\partial z} = 0 \qquad s_0(t) < z < s(t),\ t_m < t < t_1 \tag{5}$$

The degree of melting in the mushy zone can be measured by solid fraction, f ,which is related to the local temperature. It can be expressed as:

$$f = \begin{cases} 0 & T = T_f + \Delta T \\ \dfrac{T_f + \Delta T - T}{2\Delta T} & T_f - \Delta T \le T \le T_f + \Delta T \\ 1 & T = T_f - \Delta T \end{cases} \tag{6}$$

According to the definition of the solid fraction of solid in the mushy zone, f can be written as

$$f = \frac{\rho_s \varphi_s}{\rho_s \varphi_s + \rho_l \varphi_l} \tag{7}$$

In the first melting stage, eq. (7) can be simplified as

$$f = \frac{1-\varepsilon}{1-\varphi_g} \tag{8}$$

Neglecting the contribution of density, heat capacity and conductivity of gas, eq. (4) can be simplified as

$$\frac{\partial}{\partial t}\left(\frac{T_m}{f}\right) + \frac{\partial}{\partial z}\left(w\frac{T_m}{f}\right) = \alpha_p \frac{\partial}{\partial z}\left(\frac{1}{f}\frac{\partial T_m}{\partial z}\right) + \frac{h_{sl}}{c_p}\frac{1}{f}\frac{\partial f}{\partial t}$$
$$s_0(t) < z < s(t),\ t_m < t < t_1 \tag{9}$$

where subscript P represents the property of powder material.

Likewise eq. (5) becomes

$$\frac{\partial}{\partial t}\left(\frac{1}{f}\right) + \frac{\partial}{\partial z}\left(w\frac{1}{f}\right) = 0 \quad s_0(t) < z < s(t),\ t_m < t < t_1 \tag{10}$$

Equations (9-10) are subjected to the following boundary conditions

$$-(1-\varphi_g)k_p \frac{\partial T_m}{\partial z} = q^{"} \qquad z = s_0(t),\ t_m < t < t_1 \tag{11}$$

$$T_m = T_f - \Delta T \qquad z = s(t),\ t_m < t < t_1 \tag{12}$$

Energy balance at the interface of solid and mushy zone interface is

$$k_p(1-\varepsilon)\frac{\partial T_m}{\partial z} = k_s \frac{\partial T_s}{\partial z} \qquad z = s(t),\ t_m < t < t_1 \tag{13}$$

The energy equation in the unsintered zone is

$$(\rho c)_p (1-\varepsilon)\frac{\partial T_s}{\partial t} = k_s \frac{\partial^2 T_s}{\partial z^2} \qquad s(t) < z < \infty,\ t_m < t < t_1 \tag{14}$$

which is subjected to the following boundary conditions

$$T_s = T_f - \Delta T \qquad z = s(t),\ t_m < t < t_1 \tag{15}$$

$$T_s = T_i \qquad z \to \infty,\ t_m < t < t_1 \tag{16}$$

The second melting stage

When $\varphi_g = 0$, the melting comes into the second stage, Governing equation and boundary conditions in the lower part of mushy zone are the same as those in the first melting stage. According to eq. (8), solid fraction, f, at the interface of upper and lower parts equals to $1-\varepsilon$ because $\varphi_g = 0$ at this interface. Therefore, the temperature at interface between the upper and lower parts can be obtained by eq. (6), i.e.,

$$T_m = T_f + (2\varepsilon - 1)\Delta T \qquad z = s_0(t), t > t_1 \tag{17}$$

Energy equation in the upper part of mushy zone can be simplified as

$$\left(1 + \frac{h_{sl}}{2c_p \Delta T}\right)\frac{\partial T_m}{\partial t} + w_0 \frac{\partial T_m}{\partial z} = \alpha_P \frac{\partial^2 T_m}{\partial z^2}$$

$$s_0(t) < z < s_m(t), t > t_1 \tag{18}$$

which is subjected to the following boundary conditions

$$k_p \frac{\partial T_m}{\partial z} = -q'' \qquad z = s_0(t), t > t_1 \tag{19}$$

$$T_m = T_f + (2\varepsilon - 1)\Delta T \qquad z = s_m(t), t > t_1 \tag{20}$$

The energy balance at the solid and mushy zone interface is

$$\left.\frac{\partial T_m}{\partial z}\right|_{z = s_m^+} = \left.\frac{\partial T_m}{\partial z}\right|_{z = s_m^-} \qquad z = s_m(t), t > t_1 \tag{21}$$

NON-DIMENSIONAL GOVERNING EQUATIONS

Introducing the following dimensionless variables:

$$\tau = \frac{\alpha_p t}{(\alpha_p \rho_p h_{sl} / q'')^2}, \quad \theta = \frac{c_p(T - T_m - \Delta T)}{h_{sl}}, \quad Z = \frac{z}{\alpha_p \rho_p h_{sl} / q''},$$

$$S = \frac{s}{\alpha_p \rho_p h_{sl} / q''}, \quad W = \frac{w \alpha_p \rho_p h_{sl} / q''}{\alpha_p}, \quad W_0 = \frac{w_0 \alpha_p \rho_p h_{sl} / q''}{\alpha_p},$$

$$K_S = \frac{k_{eff}}{k_P(1-\varepsilon)}, \quad \Delta\theta_m = \frac{2c_p \Delta T}{h_{sl}} \tag{22}$$

the non-dimensional governing equations and boundary conditions can be obtained.

Preheating Stage

$$K_s \frac{\partial^2 \theta_s}{\partial Z^2} = \frac{\partial \theta_s}{\partial \tau} \qquad 0 \le Z < \infty, \tau < \tau_m \tag{23}$$

$$\frac{\partial \theta_s}{\partial Z} = -\frac{1}{K_s(1-\varepsilon)} \qquad Z = 0, \tau < \tau_m \tag{24}$$

$$\theta_s = \theta_i \qquad Z \to \infty, \tau < \tau_m \tag{25}$$

The first melting stage

$$\frac{\partial}{\partial \tau}\left(\frac{\theta_m}{f}\right) + \frac{\partial}{\partial Z}\left(W\frac{\theta_m}{f}\right) = \frac{\partial}{\partial Z}\left(\frac{1}{f}\frac{\partial \theta_m}{\partial Z}\right) + \frac{1}{f}\frac{\partial f}{\partial \tau}$$

$$S_m(\tau) < Z < S(\tau), \tau_m < \tau < \tau_1 \tag{26}$$

$$\frac{\partial}{\partial \tau}\left(\frac{1}{f}\right) + \frac{\partial}{\partial Z}\left(\frac{W}{f}\right) = 0 \qquad S_m(\tau) < Z < S(\tau), \tau_m < \tau < \tau_1 \tag{27}$$

$$\frac{\partial \theta_m}{\partial Z} = \frac{-f_0}{1-\varepsilon} \qquad Z = S_m(\tau), \tau_m < \tau < \tau_1 \tag{28}$$

$$\theta_m = -\Delta\theta_m \qquad Z = S(\tau), \tau_m < \tau < \tau_1 \tag{29}$$

$$\frac{\partial \theta_m}{\partial Z} = K_s \frac{\partial \theta_s}{\partial Z} \qquad Z = S(\tau), \tau_m < \tau < \tau_1 \tag{30}$$

$$K_s \frac{\partial^2 \theta_s}{\partial Z^2} = \frac{\partial \theta_s}{\partial \tau} \qquad S(\tau) < Z < \Delta, \tau_m < \tau < \tau_1 \tag{31}$$

$$\theta_s(Z,\tau) = -\Delta\theta_m \qquad Z = S(\tau), \tau_m < \tau < \tau_1 \tag{32}$$

$$\theta_s = \theta_i \qquad Z \to \infty, \tau_m < \tau < \tau_1 \tag{33}$$

where f_0 is the mass fraction of solid on the surface of powder bed.

The second melting stage

$$\left(1 + \frac{1}{\Delta\theta_m}\right)\frac{\partial \theta_m}{\partial \tau} + W_0 \frac{\partial \theta_m}{\partial Z} = \frac{\partial^2 \theta_m}{\partial Z^2} \qquad S_0(\tau) < Z < S_m(\tau), \tau > \tau_1 \tag{34}$$

$$\frac{\partial \theta_m}{\partial Z} = -1 \qquad Z = S_0(\tau), \tau > \tau_1 \tag{35}$$

$$\theta_m = (\varepsilon - 1)\Delta\theta_m \qquad Z = S_m(\tau), \tau > \tau_1 \tag{36}$$

$$\left.\frac{\partial \theta_m}{\partial Z}\right|_{Z = S_m^+} = \left.\frac{\partial \theta_m}{\partial Z}\right|_{Z = S_m^-} \qquad Z = S_m(\tau), \tau > \tau_1 \tag{37}$$

$$\frac{\partial}{\partial \tau}\left(\frac{\theta_m}{f}\right) + \frac{\partial}{\partial Z}\left(W\frac{\theta_m}{f}\right) = \frac{\partial}{\partial Z}\left(\frac{1}{f}\frac{\partial \theta_m}{\partial Z}\right) + \frac{1}{f}\frac{\partial f}{\partial \tau}$$

$$S_m(\tau) < Z < S(\tau), \tau > \tau_1 \tag{38}$$

$$\frac{\partial}{\partial \tau}\left(\frac{1}{f}\right) + \frac{\partial}{\partial Z}\left(\frac{W}{f}\right) = 0 \qquad S_m(\tau) < Z < S(\tau), \tau > \tau_1 \tag{39}$$

$$\theta_m = -(\varepsilon - 1)\Delta\theta_m \qquad Z = S_m(\tau), \tau > \tau_1 \tag{40}$$

$$\theta_m = -\Delta\theta_m \qquad Z = S(\tau), \tau > \tau_1 \tag{41}$$

$$\frac{\partial \theta_m}{\partial Z} = K_s \frac{\partial \theta_s}{\partial Z} \qquad Z = S(\tau), \tau > \tau_1 \tag{42}$$

$$K_s \frac{\partial^2 \theta_s}{\partial Z^2} = \frac{\partial \theta_s}{\partial \tau} \qquad S(\tau) < Z < \infty, \tau > \tau_1 \tag{43}$$

$$\theta_s(Z,\tau) = -\Delta\theta_m \qquad Z = S(\tau), \tau > \tau_1 \tag{44}$$

$$\theta_s = \theta_i \qquad Z \to \infty, \tau > \tau_1 \tag{45}$$

INTEGRAL APPROXIMATE SOLUTION

Preheating

To solve the preheating problem, the dimensionless thermal penetration depth is introduced, i.e. $\Delta = \delta / \alpha_p \rho_p h_{sl} / q''$, where δ is the thermal penetration depth beyond which the temperature of the powder bed is not affected by the surface heating. Integrating the heat-conduction eq. (23) with respect to Z in the interval of $(0, \Delta)$, one obtains

$$K_s\left(\frac{\partial \theta_s(\Delta,\tau)}{\partial Z} - \frac{\partial \theta_s(0,\tau)}{\partial Z}\right) = \frac{d}{d\tau}(\Theta_s - \theta_i \Delta) \tag{46}$$

where $$\Theta_s = \int_0^{\Delta} \theta_s(Z,\tau) dZ \tag{47}$$

Assuming that the temperature distribution is a second-order polynomial function and applying the boundary conditions, one obtains

$$\theta_s = \theta_i + \frac{1}{2K_s(1-\varepsilon)\Delta}(\Delta - Z)^2 \tag{48}$$

Substituting eq. (48) into eq. (46), one gets

$$\Delta = (6K_s\tau)^{1/2} \tag{49}$$

Melting occurs when the surface temperature reaches the lower limit of melting temperature range, $\theta_s = -\Delta\theta_m$. The corresponding thermal penetration depth and the duration of the preheating can be obtained, i.e.,

$$\Delta_m = -2K_s(\theta_i + \Delta\theta_m)(1-\varepsilon) \tag{50}$$

$$\tau_m = \frac{2(\theta_i + \Delta\theta_m)^2(1-\varepsilon)^2}{3K_s} \tag{51}$$

Then the dimensionless temperature distribution in the unsintered zone at time τ_m are found from

$$\theta_s(Z,\tau_m) = \theta_i - (\theta_i + \Delta\theta_m)\left(1 - \frac{Z}{\Delta_m}\right)^2 \tag{52}$$

The first melting stage

At the beginning of melting process, the interface between mushy zone and unsintered zone moves in the positive axial direction of z and the surface of the powder bed moves in the same direction due to shrinkage. At the same time, the thermal penetration depth continuously increases.

Integrating eq. (31) in the interval of (S,Δ), the integral equation of solid phase is obtained,

$$K_s\left[\frac{\partial\theta_s(\Delta,\tau)}{\partial Z} - \frac{\partial\theta_s(S,\tau)}{\partial Z}\right] = \frac{d}{d\tau}(\Theta - \theta_i\Delta - \Delta\theta_m S) \tag{53}$$

where

$$\Theta = \int_S^{\Delta}\theta_s\, dZ \tag{54}$$

Assuming the temperature distribution in the solid phase is a second-order polynomial function and determining the constants in the polynomial function yields

$$\theta_s(Z,\tau) = \theta_i - (\theta_i + \Delta\theta_m)\left(\frac{\Delta - Z}{\Delta - S}\right)^2 \tag{55}$$

Substituting eq. (55) into eq. (53), one obtains

$$\frac{6K_s}{\Delta - S} = \frac{d\Delta}{d\tau} + 2\frac{dS}{d\tau} \tag{56}$$

Integration of eq. (27) from S_m to S with respect to Z, one obtains

$$\frac{d}{d\tau}\left(\Theta_1 - \frac{1}{f}\Big|_{Z=S} S + \frac{1}{f}\Big|_{Z=S_m} S_m\right) + \frac{W}{f}\Big|_{S_m}^{S} = 0 \tag{57}$$

where

$$\Theta_1 = \int_S^{S_m}\frac{1}{f}\,dz \tag{58}$$

Integration of eq. (26) from S_m to S with respect to Z, one obtains

$$\frac{d}{d\tau}\left(\Theta_2 - \Theta_3 - \frac{\theta_m}{f}\Big|_{Z=S} S - \ln f\Big|_{Z=S_m} S_m\right) = \frac{1}{f}\frac{d\theta_m}{d\tau}\Big|_{S_m}^{S} \tag{59}$$

where

$$\Theta_2 = \int_S^{S_m}\frac{\theta_m}{f}dz \tag{60}$$

$$\Theta_3 = \int_S^{S_m}\ln f dz \tag{61}$$

The expression of solid fraction, f, as a single value of temperature in the mushy zone, eq. (6), is difficult to be used to get the solution of eq. (59) because integration in eq. (60) is hard to obtain. The effect of linear distribution of solid fraction in the mushy zone using integral method was investigated by Tien and Geiger [19] and no significant effect on the result was found. For the sake of simplicity, it is assumed that the inverse of solid fraction is a linear function in the mushy zone, i.e.,

$$\frac{1}{f} = 1 - \left(1 + \frac{\Delta\theta_m}{\theta_0}\right)\frac{S - Z}{S - S_m} \tag{62}$$

It is assumed that the temperature distribution in the mushy zone is

$$\frac{\theta_m}{f} = A_0 + A_1\left(\frac{S-Z}{S-S_m}\right) + A_2\left(\frac{S-Z}{S-S_m}\right)^2 \tag{63}$$

where θ_0 is the dimensionless temperature on the heating surface of the powder bed. Coefficients A_0, A_1, A_2 can be determined using the boundary conditions specified by eqs. (28-30).

Substituting eq. (62) into eq. (57), one obtains

$$S_m = \frac{\frac{\Delta\theta_m}{\theta_0} + 1}{\frac{\Delta\theta_m}{\theta_0} + 1}S \tag{64}$$

Substituting eqs. (62-63) into eq. (59), one obtains

$$\frac{d}{d\tau}\left[\left(A_0 + \frac{A_1}{2} + \frac{A_2}{3} + \frac{-\left(1 + \frac{\Delta\theta_m}{\theta_0}\right) + \frac{\Delta\theta_m}{\theta_0}\ln\left(-\frac{\Delta\theta_m}{\theta_0}\right)}{1 + \frac{\Delta\theta_m}{\theta_0}}\right)(S - S_m)\right]$$
$$+\left(\Delta\theta_m - \frac{(1 + \frac{\Delta\theta_m}{\theta_0})\ln\left(-\frac{\Delta\theta_m}{\theta_0}\right)}{\frac{\Delta\theta_m}{\theta_0} - 1}\right)\frac{dS}{d\tau} = \frac{2K_s(\theta_i + \Delta\theta_m)}{\Delta - S} + \frac{1}{1-\varepsilon} \tag{65}$$

The initial conditions for eqs. (56), (64), and (65) are

$$S_m(\tau_m) = 0. \tag{66}$$

$$S(\tau_m) = 0. \tag{67}$$

$$\Delta(\tau_m) = \Delta_m = -2K_s(\theta_i + \Delta\theta_m)(1-\varepsilon) \tag{68}$$

By using Runge-Kutta method we can get the solutions of eqs. (56),(64) and (65).

The second melting stage

The governing equation and boundary conditions in the unsintered zone are the same as those in the first melting stage, eq. (55) and eq. (56) still describe the temperature distribution and location of the interface between mushy zone and unsintered zone in the second melting stage.

As to the lower part of mushy zone, equations (57-61) gained in the mushy zone of the first melting process are still applicable. Using the similar method, we assume that

$$\frac{1}{f}=1+\frac{\varepsilon}{1-\varepsilon}\frac{S-Z}{S-S_m} \qquad S_m(\tau)<Z<S(\tau),\tau>\tau_1 \tag{69}$$

$$\frac{\theta_3}{f}=B_0+B_1\left(\frac{S-Z}{S-S_m}\right)+B_2\left(\frac{S-Z}{S-S_m}\right)^2 \qquad S_m(\tau)<Z<S(\tau),\tau>\tau_1 \tag{70}$$

Coefficients B_0, B_1, B_2 can be determined using the boundary conditions specified by eqs. (40-42).

Substituting eq. (69) into eq. (57), one obtains

$$S_m=\frac{2}{\varepsilon}S_0-S \tag{71}$$

Substituting eqs. (69-70) into eq. (59), one obtains

$$\frac{d}{d\tau}\left(-\frac{K_s(\theta_i+\Delta\theta_m)}{3(\Delta-S)}(S-S_m)^2-\left(\frac{\varepsilon\Delta\theta_m}{6(1-\varepsilon)}+1+\frac{\ln(1-\varepsilon)}{\varepsilon}\right)(S-S_m)\right)$$
$$+\Delta\theta_m\frac{dS_0}{d\tau}-\ln(1-\varepsilon)\frac{dS_m}{d\tau}=\frac{4K_s(\theta_i+\Delta\theta_m)}{\Delta-S}+\frac{\varepsilon(2-\varepsilon)\Delta\theta_m}{(1-\varepsilon)(S-S_m)} \tag{72}$$

As to the upper part of mushy zone, since the entire layer moves with velocity w_0, the layer is static from the coordinate, z', which moves with velocity w_0. Introducing the following variable transformation,

$$Z'=\left(Z-\int_0^\tau W_0 d\tau\right)\sqrt{1+\frac{1}{\Delta\theta_m}}=(Z-S_0)\sqrt{1+\frac{1}{\Delta\theta_m}} \tag{73}$$

$$\theta_m'=\theta_m(Z',\tau)-(\varepsilon-1)\Delta\theta_m \tag{74}$$

eqs. (34-36) can be written as

$$\frac{\partial^2\theta_m'}{\partial Z'^2}=\frac{\partial\theta_m'}{\partial\tau} \quad 0<Z'<(S_m(\tau)-S_0(\tau))\sqrt{1+\frac{1}{\Delta\theta_m}},\tau>\tau_1 \tag{75}$$

$$\frac{\partial\theta_m'}{\partial Z'}=-1 \qquad Z'=0,\tau>\tau_1 \tag{76}$$

$$\theta_m'(Z',\tau)=0 \quad 0<Z'<(S_m(\tau)-S_0(\tau))\sqrt{1+\frac{1}{\Delta\theta_m}},\tau>\tau_1 \tag{77}$$

The exact solution of eqs. (75-77) is [20]

$$\theta_m'(Z',\tau)=\frac{2\sqrt{\tau-\tau_m}}{\sqrt{1+\frac{1}{\Delta\theta_m}}}\left[ierfc\left(\frac{Z'}{2\sqrt{\tau-\tau_m}}\right)-ierfc\left(\frac{(S_m-S_0)}{2\sqrt{\tau-\tau_m}}\sqrt{1+\frac{1}{\Delta\theta_m}}\right)\right] \tag{78}$$

Changing eq.(78) back to the Z coordinate and Substituting it into eq. (37), we get

$$erfc\left(\frac{(S_m-S_0)}{2\sqrt{\tau-\tau_m}}\sqrt{1+\frac{1}{\Delta\theta_m}}\right)=\frac{2K_s(\theta_i+\Delta\theta_m)(1-\varepsilon)}{\Delta-S}+\frac{(2-\varepsilon)\varepsilon\Delta\theta_m}{S-S_m} \tag{79}$$

Equations (56),(71),(72),(79) can be solved by the Runge-Kutta method with the initial conditions gained from the first melting stage.

RESULT AND DISCUSSION

Porosity, subcooling, dimensionless thermal conductivity and the temperature range of melting play significant roles in the surface temperature, locations of the different interfaces of the powder bed.

The effect of the initial porosity in the powder bed on the surface temperature during the melting process is shown in Fig. 2. It can be seen that the surface temperature increases with the increasing porosity in the powder bed because the effective thermal conductivity decreases with the increasing volume fraction of the gas. Figure 3 shows the interface locations corresponding to the same conditions of Fig. 2. In the first melting stage, $S-S_0$ increases with the increasing time, which means S moves down faster than S_0. In the second melting stage, the moving velocity of S decreases first and then moves at the velocity close to that in the first melting stage. At the same time S_m moves down significantly faster than S_0. Thus S_m-S_0 becomes larger while $S-S_m$ becomes smaller.

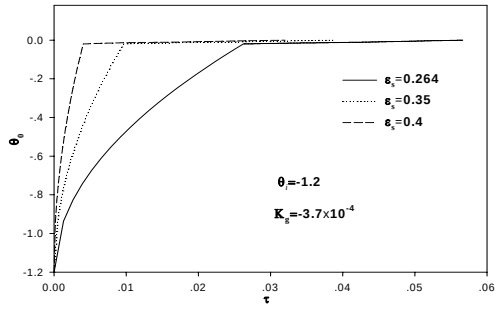

Fig.2 Effect of porosity on the surface temperature ($\Delta\theta_m=0.02$)

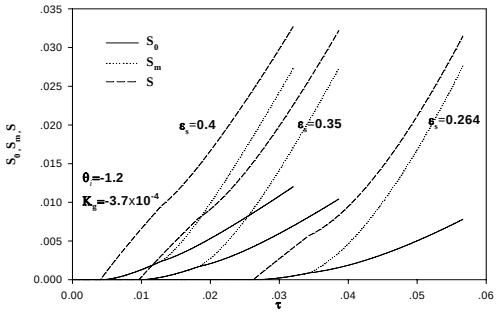

Fig.3 Effect of porosity on the interface locations ($\Delta\theta_m=0.02$)

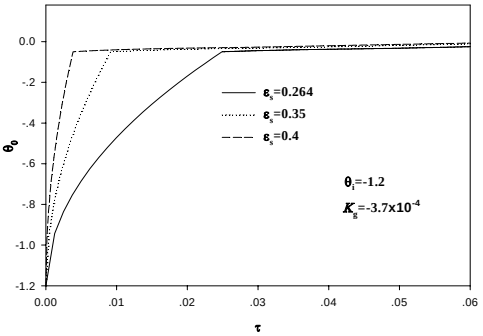

Fig.4 Effect of porosity on the surface temperature ($\Delta\theta_m=0.05$)

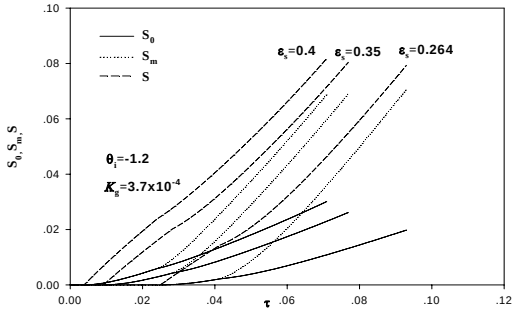

Fig.5 Effect of porosity on the interface locations ($\Delta\theta_m = 0.05$)

Figures 4-5 show the effect of initial porosity on the heating surface temperature, interface locations when $\Delta\theta_m = 0.05$. Compared with Figs. 2-3 which showed the effects of initial porosity when $\Delta\theta_m = 0.02$, it can be seen that with the increasing $\Delta\theta_m$ the preheating time becomes shorter because the powder begins to melt at a relatively lower temperature, which is earlier to be reached in the preheating process. The moving velocities of interfaces become smaller.

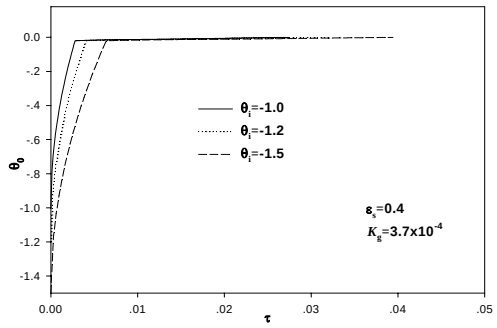

Fig.6 Effect of subcooling on the surface temperature ($\Delta\theta_m = 0.02$)

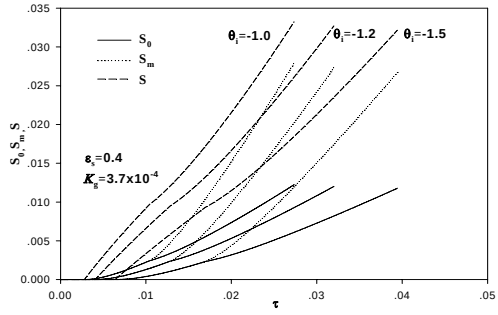

Fig.7 Effect of subcooling on the interface locations ($\Delta\theta_m = 0.02$)

Figure 6 shows the effect of initial subcooling of the powder bed on the heating surface temperature. It can be seen that the duration of preheating is increased with increasing subcooling value. The surface temperature after melting is lower for larger initial subcooling value. Figure 7 shows the interface locations corresponding to the condition of Fig. 6. As can be seen, the existence of initial subcooling reduces the moving velocities of interfaces substantially. Thickness of the layer between S_0 and S_m remains almost unchanged while thickness of the layer between S_m and S is increased with increasing subcooling value.

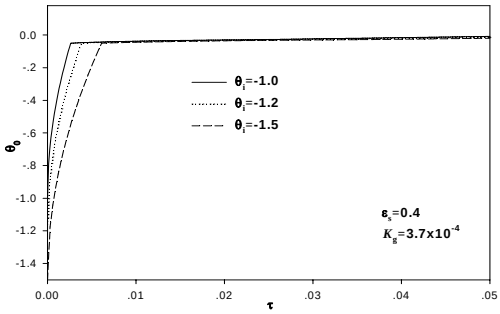

Fig.8 Effect of subcooling on the surface temperature ($\Delta\theta_m = 0.05$)

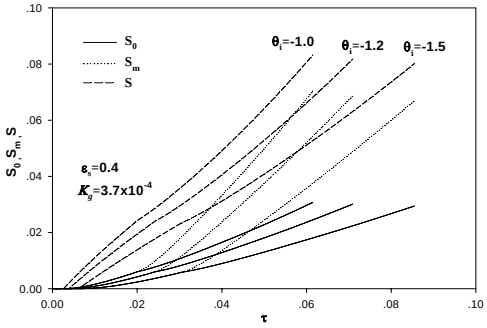

Fig.9 Effect of subcooling on the interface locations ($\Delta\theta_m = 0.05$)

Figures 8-9 show the effect of initial subcooling on the heating surface temperature, interface locations when $\Delta\theta_m = 0.05$. Compared with Figs. 6-7 which show the effects of initial subcooling when $\Delta\theta_m = 0.02$, it can be seen that with the increasing $\Delta\theta_m$ temperature on the heating surface changes more quickly, the interface locations move down faster.

Figure 10 shows the effect of dimensionless thermal conductivity of the gas on the heating surface temperature. It can be seen that the preheating time increases significantly when the thermal conductivity of the gas is increased. The surface temperature is slightly lower for higher thermal conductivity of gas.

Figure 11 shows the effect of thermal conductivity on the interface locations corresponding to the conditions of Fig. 10. As can be seen, the moving velocities of the interfaces decrease

with the increase of dimensionless thermal conductivity of gas. And the thickness of layer between S_0 and S_m remains almost unchanged while the thickness of layer between S_m and S is increased with the increase of the thermal conductivity.

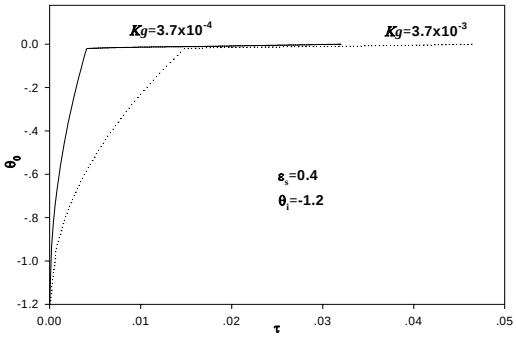

Fig.10 Effect of thermal conductivity on the surface temperature ($\Delta\theta_m = 0.02$)

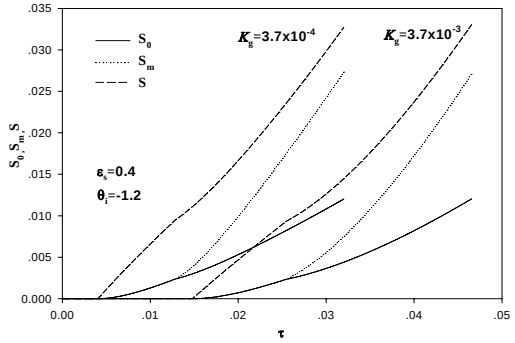

Fig.11 Effect of thermal conductivity on the interface locations ($\Delta\theta_m = 0.02$)

Figures 12-13 show the effects of dimensionless thermal conductivity of the gas on the heating surface temperature, interface locations when $\Delta\theta_m = 0.05$. Compared with Figs. 10-11 which show the effects of dimensionless thermal conductivity of the gas when $\Delta\theta_m = 0.02$, the preheating time decreases with the increase of $\Delta\theta_m$, the interface locations move down more slowly.

CONCLUSION

Melting of single-component metal powder bed subjected to constant heat flux heating is investigated analytically. Effect of shrinkage and effect of volume fraction of gas during the melting process are taken into account in the model presented in this article. It shows the porosity of the powder bed, subcooling parameter and dimensionless thermal conductivity and the temperature range of melting play important roles in the surface temperature, the locations of the interfaces and their motions. Under the condition of fixed range of melting temperature, the initial porosity of the powder bed accelerates the melting process and increases the surface temperature. The initial subcooling of the powder bed decelerates the melting process and decreases the surface temperature and decelerates the driving process of gas in the mushy zone. It also shows that the thermal conductivity of the gas slows down the melting process, decreases the heating surface temperature.

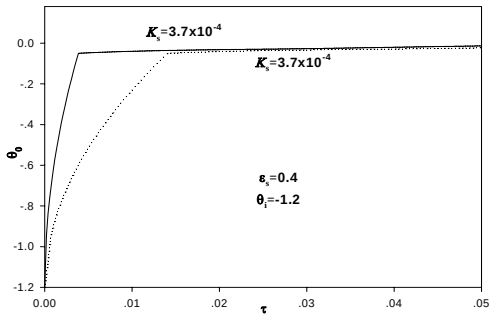

Fig.12 Effect of thermal conductivity on the surface temperature ($\Delta\theta_m = 0.05$)

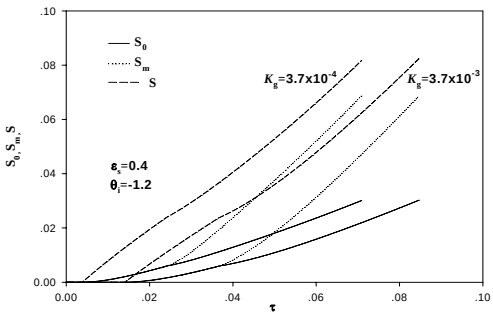

Fig.13 Effect of thermal conductivity on the interface locations ($\Delta\theta_m = 0.05$)

ACKNOWLEDGMENTS

Support for this work by the office of Naval Research (ONR) under grant number N00014-04-1-0303 is greatly acknowledged.

REFERENCES

[1] Agarwala, M., Bourell, D., Beaman, J., Marcus, H. and Barlow, J., 1995, "Direct selective laser sintering of metals," Rapid Prototyping Journal, Vol. 1, pp. 26-36.

[2] Das, S., Beaman, J. J., Wohlert, M. and Bourell, D. L., 1998, "Direct laser freedom fabrication of high performance metal components," *Rapid Prototyping Journal*, Vol. 4, pp. 112- 117.

[3] Zong, G., Wu, Y., Tran, N., Lee, I., Bourell, D. L., Beaman, J. J. and Marcus, H. L., 1992, " Direct solid freedom fabrication of high temperature materials," *Proceedings of a*

symposium on Processing and Fabrication of Advance Materials forHigh Temperature Applications, in Ravi, V. A. and Srivatsan, T. S.(Eds), TMS, Warrendale, PA, pp. 503-518.

[4] Lu, L., Fuh, J. and Wong, Y. S., 2001, *Laser-induced material and processes for rapid prototyping*, Kluwer Academic Publishers, Boston, MA.

[5] Prabhu, G. and Bourell, D. L., 1993, "Supersolidus liquid phase sintering of prealloyed bronze powder," *Proceeding of the Solid Freeform Fabrication Symposium*, Beaman, J. J., Marcus, H. L., Bourell, D. L. and Barlow, J. W. (Eds), The University of Texas at Austin, Austin, TX, 1993, pp. 193-202.

[6] Simichi, A., Petzoldt, F. and Pohl, H., 2001, "Direct metal laser sintering: material considerations and mechanisms of particle bonding", *International Journal of Powder Metallurgy*, 37, No.2, pp. 49-61.

[7] Manriquez-Frayre, A. and Bourell, D. L., "Selective laser sintering of binary metallic powder," *Proceeding of the Solid Freeform and Fabrication Symposium*, Beaman J. J., Marcus, H. L., Bourell, D. L. and Barlow, J. W. (Eds), The University of Texas at Austin, Austin, TX, 1994.

[8] Zhang, Y. and Faghri, A., 1998, "Melting and re-solidification of a sub-cooled mixed powder bed with moving Gaussian heat source," *ASME Journal of Heat Transfer*, Vol. 120, pp. 883-891.

[9] Zhang, Y. and Faghri, A., 1999, "Melting of a subcooled mixed powder bed with constant heat flux heating," *International Journal of Heat and Mass Transfer*, Vol. 42, pp. 775-788.

[10] Zhang, Y., Faghri, A., Buckely, C. W. and Bergman, T. L., 2000, "Three-dimensional sintering of two-component metal powders with stationary and moving laser beams," *ASME Journal of Heat Transfer*, Vol. 122, No. 1, pp 150-158

[11] Meiners, W., Over, C., Wissenbach, K., Poprawe, R., 1999, "Direct generation of metal parts and tools by selective laser powder remelting(SLPR)," *Proceedings of 1999 Solid Freeform Fabrication Symposium*, pp 655-662.

[12] Hauser, C., Childs, T. H. C., Dalgarno, K. W., and Eane, R. B., 1999, "Atmospheric Control During Direct Selective Laser Sintering of Stainless Steel 314S Powder," *Proceedings of Solid Freeform Fabrication Symposium 1999*, pp. 265-272.

[13] Hauser, C., Childs, T. H. C., and Dalgarno, K. W., 1999, "Selective Laser Sintering of Stainless Steel 314S HC Processed using Room Temperature," *Proceedings of Solid Freeform Fabrication Symposium 1999*, pp. 273-280.

[14] Miani, F., 2000, "On the Development of New Metal Powders for the Selective Laser Sintering Process," Proceedings of the Third World Congress on Intelligent Manufacturing Process and System, Boston, MA.

[15] Morgan, R., Sutcliffe, C. J., and O'Neill, W., 2001, "Experimental Investigation of Nanosecond Pulsed Nd:YAG Laser Re-melted Pre-placed Powder Beds," *Rapid Prototyping Journal*, Vol.7, pp. 159-172.

[16] Karapatics, N., Egger, G., Gygax, P. E., and Glardon, R., 1999, "Optimization of Powder Layer Density in Selective Laser Sintering," *Proceedings of Solid Freeform Fabrication Symposium 1999*, pp. 255-263.

[17] Viskanta, R., 1983, *Solar Heat Storage: Latent Heat Materials*, CRC Press, FL.

[18] Yao, L. C. and Prusa, J., 1989, "Melting and freezing," *Advances in Heat Transfer*, **25,** pp. 1-96.

[19] Tien, R. H., and Geiger, G. E., 1967, "A heat-transfer analysis of the solidification of a binary eutectic system," *ASME J. Heat Transfer*, Vol. 91, pp. 230-234.

[20] El-Genk, M. S., Cronenberg, A. W., 1979, Solidification in a semi-infinite region with boundary condition of the second kind: an exact solution, *Letters in Heat and Mass Transfer*, Vol. 6, pp. 321-327.